Anderson localization in the time domain: Numerical studies of waves in two-dimensional disordered media

R. L. Weaver
Theoretical and Applied Mechanics, University of Illinois, Urbana, Illinois 61801
(Received 8 April 1993; revised manuscript received 7 September 1993)

A numerical model for the dynamics of a classical wave equation in a two-dimensional Anderson disordered medium is integrated over times of the order of 27 000 inverse bandwidths. Excitations by narrow band sources lead to wave energy densities whose ensemble averages behave diffusively at early times. The behavior at more general times and distances is, however, not diffusive. The observed transport profiles are shown to be inconsistent with predictions from a simple hydrodynamical continuum model of Anderson localization, and to the hypothesis of exponentially slow diffusion. The evolution of the energy density distribution in systems with varying disorders and microstructures, and over a range of length scales, is found to collapse to a single function of rescaled space and time well approximated by $e(x,t)\approx\exp\{-x/\xi-(x^{2+n}/4\beta\xi^n t)^p\}$ with $n\approx 0.46$, $p\approx 0.76$, where x is the distance from the source, ξ is the localization length, and the β is a "residual diffusivity" not equal to the bare diffusivity. Dissipation is shown to have no delocalizing effect.

I. INTRODUCTION

Classical wave systems resemble their electronic counterparts in many ways. Amongst the significant differences one may count the lack in electronic systems of a true analog to dissipation, and the lack in most classical systems of significant inelastic processes in which waves may change their frequency or lose temporal phase information. Nevertheless, the purely wave aspects are very similar. Hence it has been anticipated for some time now that classical waves should localize in sufficiently disordered media.[1-9] Indeed because of difficulties controlling electron-electron interactions and in controlling the rate of inelastic processes, the electronic metal-insulator transition is now understood to be a poor example of Anderson localization. In order to better isolate the effects of disorder, and to study the Anderson transition with less obscuration by electron interactions and inelastic processes, a search for localization of classical waves is in progress.[10-15] In such systems one could conceivably better control nonlinearity and inelastic scattering rates.[13] Furthermore, in such systems one potentially has access to time-domain behavior and to new physical phenomena related to the different types of wave equations.

As long anticipated,[1,2] recent experimental work attempting to demonstrate anomalous diffusion and Anderson localization of classical waves, in the electromagnetic[10,11,15] and acoustic[12-14] cases, has concluded with various ambiguities because dissipation has obscured the transition. As recently emphasized, however,[16] dissipation does not cause the otherwise localized eigenfunctions to become extended, but merely enhances the sensitivity of certain types of measurements to the short-time scales on which anomalous diffusion may be less manifest. In a measurement conducted in the time domain, however, such as that of Ref. 12, or in a measurement of frequency-frequency correlations such as that of Refs. 10 and 11, the experimentalist can hope to distinguish the effects of dissipation from those of anomalous diffusion. Indeed this access to the time domain is one of the attractions to the study of classical wave localization.

In carrying out such work, however, the experimentalist has been put at a disadvantage by the lack of theory for time-domain behavior. Genack and Garcia's[10,11] analysis of microwave transmission through a system of aluminum and polystyrene balls was based in part upon the notion that transport in a sufficiently dissipative but otherwise localizing system would appear fully classically diffusive. A reanalysis of experiments such as these requires that we replace that model with a correct one. It is the intention of the present communication to present evidence for the behavior of anomalous wave transport in the time domain that could, ultimately, be used to generate a more precise model and thereby inform the interpretation and reanalysis of experiments like these.

The theory of anomalous wave transport in the time domain is not well developed. There is very little discussion of generalizations of the diffusion equation Green's function, or generalizations of the diffusion equation itself, appropriate for an Anderson localizing medium. White *et al.*[17] have presented a few results for one-dimensional systems. Abrahams and Lee[18] considered the electron dielectric function's q and ω dependence in $2+\varepsilon$ dimensions near the mobility edge. Presumably because there is no edge in two dimensions, their expressions become indeterminate at $\varepsilon=0$. A simple hydrodynamical model of a particle diffusing under the influence of a restoring force has been shown[19] to generalize classical diffusion to the diffuse transport of a localizing quantity. As will be seen in this paper, however, that model does not describe observations. The goal of the present project, of which this paper is a part, is to discover the correct function.

Experimental work in the time domain on Anderson localization and anomalous diffusion in dimensions greater than one is confined to the work by Weaver,[12] and, inasmuch as measurements of frequency-frequency intensity correlation functions imply measurements of time-domain behavior, that of Genack and Garcia.[10,11] Numerical work in the time domain is reported by Prelovsek,[20] Scher,[21] Shore and Halley,[22] Weaver and Loewenherz,[23] Weaver,[16] and Vanneste, Sebbah, and Sornette.[24] None of these studies have been conducted with sufficient detail for the unambiguous determination of the effective transport behavior. In Refs. 20, 21, and 23 the sole interest was the evaluation of the mean-square displacement $\langle R^2(t)\rangle$ of the diffusing particle. $\langle R^2(t)\rangle$ is related to the second moment of a more fundamental quantity: the particle (or energy in a classical wave system) density $e(\mathbf{r},t)$ as a function of space and time. Weaver[16] presented numerical studies in order to demonstrate the incorrectness of the usual hypothesis regarding the effect of dissipation upon $e(\mathbf{r},t)$, but he did not attempt to quantitatively characterize the function. Recent experiments measuring e in two-dimensional ultrasonic system[12] were marred by the action of unknown agents which seemed to deenhance the localization and made quantitative conclusions difficult. One of the few firm conclusions, other than that the system did exhibit localization, was that the fit of $e(\mathbf{r},t)$ to the predictions of the simple hydrodynamical model[19] was poor. While time-domain behavior is implicitly addressed by Genack and Garcia,[10,11] that work measures only one time-domain parameter, the width of the photon time-of-flight distribution. Shore and Halley[22] numerically investigated the time-domain response of the electron current in a small three-dimensional Anderson model to a step voltage change. The samples considered were small, however, and interest restricted to the earliest times. Thus very little is known about the time-domain behavior of anomalous wave transport.

This paper will present results obtained from numerical experiments in an attempt to rectify this lack. In the following section a numerical model is introduced which allows the tracking of evolving wave energy density in a two-dimensional classical wave equation version of an Anderson model disordered Hamiltonian. The behavior of the evolving wave energy density at short times and distances is discussed in Sec. III. The results there are compared to the predictions of a classical diffusion equation and used to extract values for the bare diffusivity. The moderate- and long-time behavior at all distances is presented in Sec. IV and shown to be independent, within a temporal rescaling, of disorder, and independent, after a further rescaling, of distance from the source. An analytic form is proposed for the resulting general function of time and distance from the source. Section V introduces a non-Anderson model disordered system for which the behavior is identical thereby suggesting that the observed energy evolution profiles have some universal character. The energy density evolution is shown in Sec. VI to be incorrectly described by a simple hydrodynamical continuum model, and in Sec. VII to be only trivially modified in the presence of dissipation. The paper concludes with a summary and some recommendations for further work.

II. NUMERICAL MODEL

The classical dynamics of an undamped two-dimensional $V=1$ Anderson model may be described by the following equation of motion:

$$\partial^2 v_{\mathbf{n}}/\partial t^2 + k_{\mathbf{n}} v_{\mathbf{n}} - \sum v_{\mathbf{m}} = F_{\mathbf{n}}(t) , \tag{1}$$

or, in matrix notation

$$\partial^2 \underline{v}(t)/\partial t^2 + \underline{\underline{K}}\,\underline{v}(t) = \underline{F}(t) , \tag{2}$$

where the bold index $\mathbf{n}$ runs over the sites of a large square lattice. The sum is over the four nearest-neighbor sites $\mathbf{m}$ of site $\mathbf{n}$, and $k_{\mathbf{n}}$ is 5 plus a random number taken from the uniform distribution $[0,W]$. The frequency domain version of (1) is, neglecting F, precisely equivalent to the tight-binding Anderson model. It has identical eigenfunctions. The eigenfrequencies differ, but in a smooth fashion. The difference in eigenfrequencies is an inevitable consequence of going to a classical model. As described below, and for a narrow-band disturbance, the difference is unimportant.

Equation (1) represents a forced classical version of an Anderson model. It may also be understood as an exact description of the transverse dynamics of a planar array of masses and random springs coupled by in-plane inertialess strings with uniform tension and driven by an external force F. Alternatively, (1) may be thought of as a spatially discrete version of a classical wave equation for a tensioned membrane on a random elastic foundation.

Equation (1) may be made to look like the Schrödinger equation by letting v be of the form

$$v_{\mathbf{n}} = \mathrm{Re}[\psi_{\mathbf{n}}(t)\exp\{i\Omega t\}] , \tag{3}$$

where Ω is a constant equal to the mean frequency of the narrow-band disturbance and $\underline{\psi}(t)$ is complex and slowly varying. With this substitution the unforced version of Eq. (1) becomes

$$2i\Omega\partial\psi_{\mathbf{n}}/\partial t - \Omega^2\psi_{\mathbf{n}} + \partial^2\psi_{\mathbf{n}}/\partial t^2 = \sum_{\mathbf{m}} K_{\mathbf{nm}}\psi_{\mathbf{m}} . \tag{4}$$

Neglecting $\partial^2\psi/\partial t^2$ compared to $\Omega\partial\psi/\partial t$, one recovers a spatially discrete Schrödinger equation:

$$2i\Omega\partial\underline{\psi}/\partial t = [\underline{\underline{K}} + \Omega^2]\underline{\psi} . \tag{5}$$

The evolution of systems like that of Eq. (5) from specified narrow-band initial conditions has been studied previously.[20,21] In this work we numerically study the evolution dictated by Eq. (1) rather than, like Prelovsek[20] and Scher,[21] Eq. (5). While the two systems must have behaviors under narrow-band excitations that are roughly equivalent, Eq. (1) has a few virtues which recommend it. Amongst these is its ready generalization to damped systems,[16] its interpretation as a spatially discrete version of a classical wave equation, and the efficiency with which it can be implemented in a conditionally stable central difference scheme.

Solutions of Eq. (1) are obtained here for systems with widths of the order of 100 or more and lengths of the order of 200. These dimensions have been chosen sufficiently large that the boundaries are expected to be unimportant. In estimating the required sizes, the conclusions of McKinnon and Kramer,[25] in which similar systems were investigated for their localization lengths, were employed. In practice a width (or circumference, as the strip has periodic boundary conditions across its width) of at least 14 times the localization length was used, thereby ensuring that the localization lengths in the strip of finite width are within a couple of percent of the localization lengths in a strip of infinite width. Constraints on numerical resources, therefore, required that the systems investigated have sufficiently short localization lengths. On the other hand, localization lengths comparable to the mesh spacing do not allow much resolution of behavior on length scales comparable to or shorter than ξ. Therefore the following cases were studied: $W/V=11$, 10, 9, and 8 with, according to McKinnon and Kramer,[25] localization lengths of $\xi=4.22$, 5.451, 7.296, and 11.07, respectively.

The excitations $F(t)$ were taken to be tone bursts applied uniformly across the width, on the central row of the mesh.[26] Boundary conditions were taken to be periodic in the width direction and fixed at the far extremities in the length direction. The systems may therefore be pictured as meshes in the shape of long cylinders with excitations applied to the central ring.

For the most part the data to be presented here are taken from points well removed from the edges, at distances greater than 5.5ξ from the ends. Thus the influence of the ends may be expected to be of order $\exp(-11)$ or less. The large system circumferences ($\sim 14\xi$) are such that one would anticipate the minor contribution from helical ray paths to arrive late, delayed relative to direct paths by a time of order $(14\xi)^2/D$, and to be diminished in importance by a factor of order $\exp\{[(x/\xi)^2+196]^{1/2}-(x/\xi)\}$ relative to the direct path. One would therefore surmise that the effects of the finite geometry are slight and that the data to be presented are representative of those corresponding to an infinite medium. This surmise has been confirmed by comparison of results obtained in systems of different sizes.

Equation (1) was solved by central differences with a time step δt chosen short enough to ensure numerical stability and to ensure that the results are in rough approximation to those that would be obtained if the time step were infinitesimal.

$$\underline{v}(t+\delta t)-2\underline{v}(t)+\underline{v}(t-\delta t)=[-\underline{\underline{K}}\,\underline{v}(t)+\underline{F}](\delta t)^2 . \quad (6)$$

This difference equation is stable if $2/\delta t$ is greater than the square root of the largest eigenvalue of $\underline{\underline{K}}$. A sufficient condition is then $\delta t<2(9+W/V)^{-1/2}$. In the cases presented here δt was set to $(9+W/V)^{-1/2}\approx 0.23$. Inasmuch as the eigenfunctions of the system (the eigenvectors of $\underline{\underline{K}}$) are independent of the temporal differencing, the precise choice of time step size is expected to be unimportant; such was indeed found to be the case. The resulting energy density was averaged in the width direction (parallel to the line source) and monitored as a function of time and distance from the source. Thus the evolution is quasi-one-dimensional. However, a presumption of isotropy in the transport properties and sufficient width in the strips studied allow the present calculations to be relevant to fully two-dimensional evolutions. Furthermore, the use of a line source rather than a point source, and the averaging of responses along lines parallel to the source, reduce the need for configuration averaging. They consequently lower the computational burden below that which would be needed for a study of the evolution from a point source.

The calculations were carried out at single precision (four bytes per floating point number) on a Hewlett-Packard Apollo 9000/750 workstation. The accuracy of the numerical implementation of Eq. (6) was checked in several ways. To within a well understood bounded fluctuation[27] the total energy—integrated over all space—was found to be independent of time. A few calculations of responses in single realizations from the ensemble were repeated at double precision. All other parameters were unchanged including the random number generator seed. All differences, at all times and distances of interest, were found to be confined to less than a part in 10^3. The code was also implemented on a Convex C240. Results on the two machines differed negligibly. The code on the Apollo was run with and without the use of vector library subroutines that used the multiple processors and with and without compiler option optimizers, also without notable differences in the results. One concludes that the numerical implementation of (6) appears accurate.

The cosine-bell tone burst sources were taken to have their central frequency such that the modes at the band center would be most excited. This allows comparisons with the band center localization lengths reported by McKinnon and Kramer. If one anticipates that the modes at the band center are the least localized and therefore the localization length is maximal there, one would conclude that a narrow band of energies at the band center would have a nearly uniform set of localization lengths, leading to little or no dispersion in transport properties, and ease in the interpretation of the numerical results. If one wishes to excite the modes at the band center, however, one must recognize that the distortion in eigenfrequencies induced by the finite temporal step size δt will cause a mode at the band center with an eigenvalue of $\underline{\underline{K}}$ equal to $(5+W/2)$ and thus an *actual* frequency [in Eq. (1)] of $(5+W/2)^{1/2}$ to have an *apparent* frequency [in Eq. (6)] of $(2/\delta t)\arcsin[(\delta t/2)(5+W/2)^{1/2}]$. Therefore this latter quantity was chosen as the central frequency of the tone burst. The band width of the tone burst source is related to its duration. The thirty cycle cosine bell tone bursts used have widths (frequency difference between half power points) of 5% of the central frequency. A longer tone burst would more sharply define the frequency of the disturbance and presumably correspondingly imply more sharply defined transport properties, but would also degrade the temporal resolution of the numerical experiments. It would in addition exacerbate statistical fluctuations across the ensemble, and in the absence of extra ensemble averaging, degrade accuracy. Tone burst lengths were chosen at 30

TABLE I. Parameters describing the properties of the five systems considered, $W/V=8$ through 11 of the Anderson model and $W=31$ in the nonAnderson model. The parameters are localization length ξ, modal density in units of modes per site per apparent circular frequency, ρ, bare diffusivity D_0, residual diffusivity β, and the apparent anomalous dimensions n and p.

W	ξ	ρ	D_0	β	n	p
8.0	11.07[a]	0.584	0.128	0.159	0.51	0.76
9.0	7.296[a]	0.543	0.105	0.152	0.50	0.76
10.0	5.451[a]	0.521	0.094	0.145	0.50	0.74
11.0	4.22[a]	0.490	0.081	0.148	0.51	0.74
31.0	6.0	0.235	0.207	0.276	0.42	0.74

[a]Localization lengths taken from Ref. 25.

cycles in an attempt to make compromises between conflicting requirements. The consequent 5% bandwidths may be compared to bandwidths of the order of 35% in Weaver's ultrasonic experiments[12] and the order 3% widths used in Genack and Garcia's[10,11] studies of time-domain behavior by means of frequency-frequency correlation functions.

In order to ascertain the modal density of the meshes considered, small (10×10, or 100 degree-of-freedom) versions of these meshes with periodic boundary conditions in both directions were analyzed for the square roots of the eigenvalues of the corresponding matrices $\underline{\underline{K}}$. For each W/V case the accumulated modal density was averaged over 20 such meshes and fit to a fifth-order polynomial function of frequency from which the slope at the band center [at $\omega=(5+W/2)^{1/2}$] was taken. The average over 25 configurations at $W/V=8$, is shown in Fig. 1. This process was repeated five times, and the observed variation takes as a measure of the accuracy of the analysis. The variations were such that one estimates these modal densities to be (one σ) accurate to within about 1%. The slight difference between *apparent* frequencies in a central differencing realization of a differential equation and the *actual* frequencies one would find if one used infinitesimal time steps requires us to rescale the system spectrum (the square roots of the eigenvalues of $\underline{\underline{K}}$) to the spectrum relevant to a finite time step solution of the differential equation. This was done by converting modal density per actual circular frequency to modal density per apparent circular frequency by multiplying by $\partial\omega_{\text{actual}}/\partial\omega_{\text{apparent}}=[1-\{\delta t/2\}^2(5+W/2)]^{1/2}$. The results are shown in Table I.

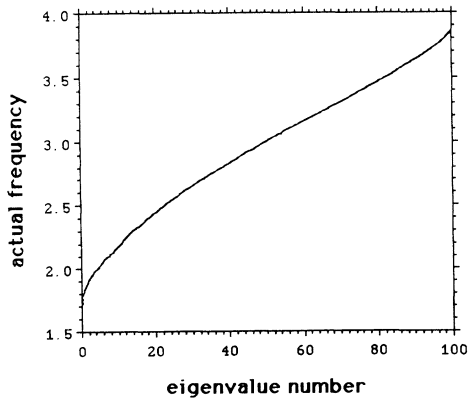

FIG. 1. The spectrum of a 10×10 periodic boundary condition Anderson model at $W/V=8$ averaged over 25 realizations from the ensemble is plotted. The eigenvalue number may be fit to a fifth-order polynomial in frequency, and the modal density at any frequency near the band center evaluated from the slope of that polynomial.

III. BEHAVIOR OF THE ANDERSON MODEL ON SHORT LENGTH AND TIME SCALES

On short-time scales the effective behavior is expected to be classically diffusive. In order to determine the effective diffusivity on these scales, the second spatial moment of the energy: $E_2(t)=\int e(x,t)x^2dx$ and the total energy as well: $E_0(t)=\int e(x,t)dx$ are calculated where $e(x,t)$ is the average energy density at a distance x from the source. e is calculated by ensemble and circumferentially averaging a local energy density at site $\mathbf{m}$ and time t defined by

$$e_{\mathbf{m}}=(1/8)|v_{\mathbf{m}}(t+\delta t)-v_{\mathbf{m}}(t-\delta t)|^2/(\delta t)^2 + (1/2)k_{\mathbf{m}}|v_{\mathbf{m}}|^2+(1/4)\sum_{\mathbf{n}}|v_{\mathbf{m}}-v_{\mathbf{n}}|^2 , \quad (7)$$

where the sum over $\mathbf{n}$ is a sum over nearest neighbors. Scher[21] and Prelovsek[20] and Loewenherz and Weaver[23] have made similar numerical calculations, defining $R^2(t)=E_2/E_0$, and studying its long-time behavior. In a localizing system R^2 should asymptote at late times at a value of order ξ^2.

In a classically diffusing system R^2 should grow linearly with time with a proportionality which is essentially the diffusivity. In this section, therefore, the short time behavior of E_2 and E_0 is studied and used to determine the effective bare diffusivity. At times after the forcing has ended such that E_0 is constant[27] one expects a classically diffusing system to have an R^2 which is linear in time; $dR^2/dt=2D_0$. In Fig. 2 an ensemble average of E_0 and the ratio of ensemble averages of E_2 and E_0 are plotted.

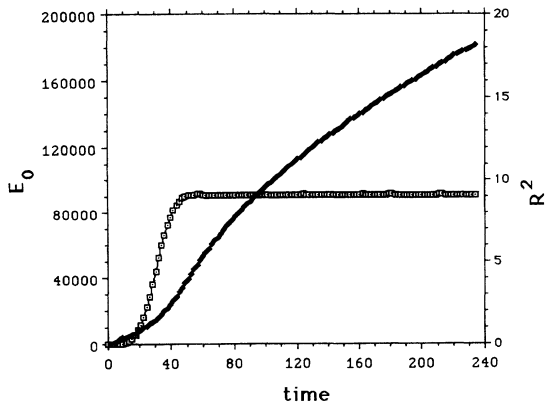

FIG. 2. The total energy and its second spatial moment are plotted versus time for the case $W/V=9$. Note that the mean energy deposition time is at $t\approx30$ on this scale. All subsequent analyses will use this moment as their zero of time.

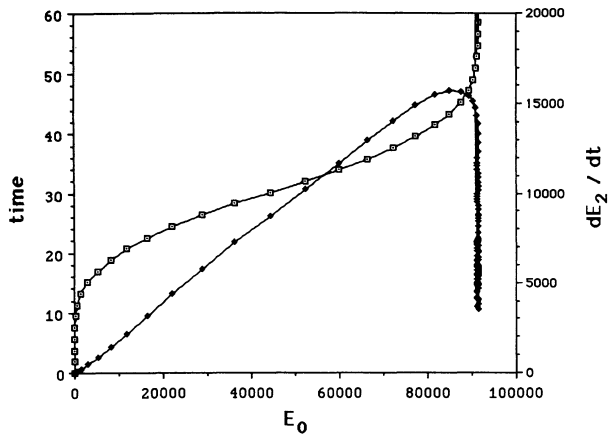

FIG. 3. The data of Fig. 2 are replotted in order to better emphasize the classical diffusion at early times.

ted versus time for the case $W/V=9$. For this case the averages were conducted over 100 configurations of systems of length 61 and width 50. Note in particular the extended period over which the total energy E_0 is rising while the 30 cycle tone burst excitation operates. R^2 shows a interesting early growth (near times $t\approx 8$) which slows almost immediately; this behavior is ascribed to ballistic propagation over length scales of order one lattice spacing. One also may note that the rise in R^2 shows a tendency to slow at times $t>60$; this is the first sign of localization which at later times would manifest as an asymptotically constant value of R^2 of the order of ξ^2. As can be seen in the figure, there is no significant region in time after which the forcing has ceased, and before which the localization is apparent. An accurate value for D_0 is, therefore, not easily extracted from a plot like that of Fig. 2. In order to obtain D_0, we plot dE_2/dt versus E_0. Classical diffusion predicts a linear slope: $dE_2/dt=E_0 2D_0$ at all times. Such a plot is shown in Fig. 3, and D_0 is readily determined from it. At early times, before the localization is felt, the plot is linear, in accord with the predictions of classical diffusion. Table I shows the D_0 values determined from the secant slopes of plots such as this at moderate times.

The energy deposition acts over a finite time interval, the peak rate of which occurs at about $t=30$. All values of time reported in the remainder of this communication will correspond to the amount of time since the instant of peak deposition.

IV. BEHAVIOR OF THE ANDERSON MODEL ON MODERATE AND LONG TIME SCALES

On moderate- and long-time scales the behavior is not classically diffusive. To demonstrate this, and with a view towards elucidating the manner in which diffuse wave energy is transported, the current work reports the results integration of Eq. (6) over long length and time scales. For the four different Anderson systems at $W/V=8$, 9, 10, and 11, solutions were generated for 250, 350, 600, and 1000 configurations of systems of size 299×143, 281×103, 217×81, and 171×63, respectively, all to about 10^5 time steps. The computations required about 7×10^{12} floating point operations at each value of W/V. The reported energies are averages, in space along a circumferential line parallel to the line source, and across the ensemble as well. Inasmuch as the process studied was a narrow, but not infinitesimal, band process, they are averages in frequency as well. It is the energies that are averaged, not their logarithms. There is reason to believe that transport strengths are not distributed normally (e.g., Refs. 10 and 11), that geometric means may be more appropriate, and that arithmetic averages of energies converge slowly. The experiments of Weaver[12] and of Genack and Garcia,[10,11] however, have reported the arithmetic means of energies and so the work here confines itself to such.

Errors in the reported average energies due to the finite configuration averaging were estimated by observing variances across the ensemble. Observed standard deviations were all within 100% of the observed mean energies except at extremes of disorder and time and distance from the source where fluctuations occasionally reached 200%. For the smaller values of W/V fluctuations were more generally in the 30–80% range. One σ error bars in the logarithms of the measured average energy densities may be estimated by dividing the standard deviations by the square root of the number of configurations used in the average. This procedure reveals that the data in the figures corresponding to $x\leq 8\xi$ may be taken to have 1 σ error bars no larger than ± 0.06.

Time is measured in the units implied by Eq. (1). The units may be converted to the inverse bandwidth units that are sometimes used to describe solutions of equations like (5) by multiplying by 8 (the Schrödinger equation bandwidth) and dividing by $2\Omega\approx 6.5$ [from Eq. (5)]. Thus the evolutions reported here over a period of the order of 23 000 in the present units correspond to about 27 000 inverse Schrödinger equation bandwidths.

In the following subsection the average energies are shown as functions of distance in order to reveal length scales in the energy distribution. R^2 is then examined at late times in order to compare with theoretical expectations for conductivity on long time scales. In the remaining subsections the temporal behavior at each of several distances from the source is studied. In Sec. IV C, the behavior is studied versus the natural logarithm of time, and the curves there found to collapse to a single curve after the application of rescalings in time. In Sec. IV D the behavior is studied versus the inverse of time in order to make comparisons with classical diffusion. In Sec. IV E the behavior is studied versus an inverse fractional power of time and found to be linear, leading to a simple approximate form for the evolution of energy density in an Anderson localizing system.

A. Spatial profiles

For each of the four different degrees of disorder ($W/V=11$, 10, 9, and 8) the average energy density profiles are shown in Figs. 4(a)–4(d) at each of several values of time. Most noteworthy in all these figures is the late time exponential form; $e(x,t)\approx\exp(-|x|/\xi)$ in ac-

cord with expectations of exponential localization. This behavior is, though, modified at short distances, where there appear to be other length scales, and at large distances for which the asymptotically late time energy density has not yet been achieved. Estimates for localization lengths might be constructed by fits to exponentials. In such a fit it would be necessary to exclude the short distances on which there are length scales other than ξ. One might also exclude the largest distances, for which asymptotic times have not been reached, but as will be shown later in this communication, there exist plausible methods for extrapolation to infinite time. These extrapolations allow one to estimate the apparent localization length at all sufficiently large x.

The extrapolations reveal that ξ_{observed}, defined as $-\lim_{(t\to\infty)}(\partial \ln e/\partial x)^{-1}$, varies with x, lengthening at large x. Near $x\approx 2\xi$, one finds ξ_{observed} to be equal within experimental uncertainties to the localization lengths reported by McKinnon and Kramer.[25] Near $x\approx 8\xi$ one finds that the observed localization lengths can be as much as 20% greater than those reported by McKinnon and Kramer. The discrepancy is not convincingly ascribable to the temporal extrapolation. Nor is it likely to be explained by the finite circumference, as finite circumference shortens the effective localization lengths.[25] The most likely cause is the finite disturbance bandwidth. In studies not displayed here ξ has been found to vary in the frequency regime near the band center. Frequencies slightly below band center have been found to be less localized than those at or above the band center. The hypothesis that ξ would be a maximum at the band center is apparently invalid. In disturbances like the ones employed here consisting of energies with a distribution of frequencies, and consequent distribution of localization lengths, the energy density at the larger distances will be dominated by the components with the slower spatial decays. For the purposes of the present work this dispersion in localizations lengths is not problematic. If future work finds it so it may be advisable to excite the system at frequencies at which ξ is stationary.

At distances within one localization length of the source there is a region of enhanced energy density. An expanded view of this region is shown in Fig. 5 for the case $W/V=9$. Close scrutiny indicates, in all four cases, that the energy density at the position of the line source at $x=0$ is about 3.2 times that which one would anticipate based upon extrapolation of the energy density profiles from the larger x. The width of the region as characterized by the position at which the energy density enhancement is only $\sqrt{3.2}$ varies with W/V. At $W/V=11$, 10, 9, and 8 the widths are estimated to be 1.8, 2.0, 2.5, and 3.2, respectively. One might wish to as-

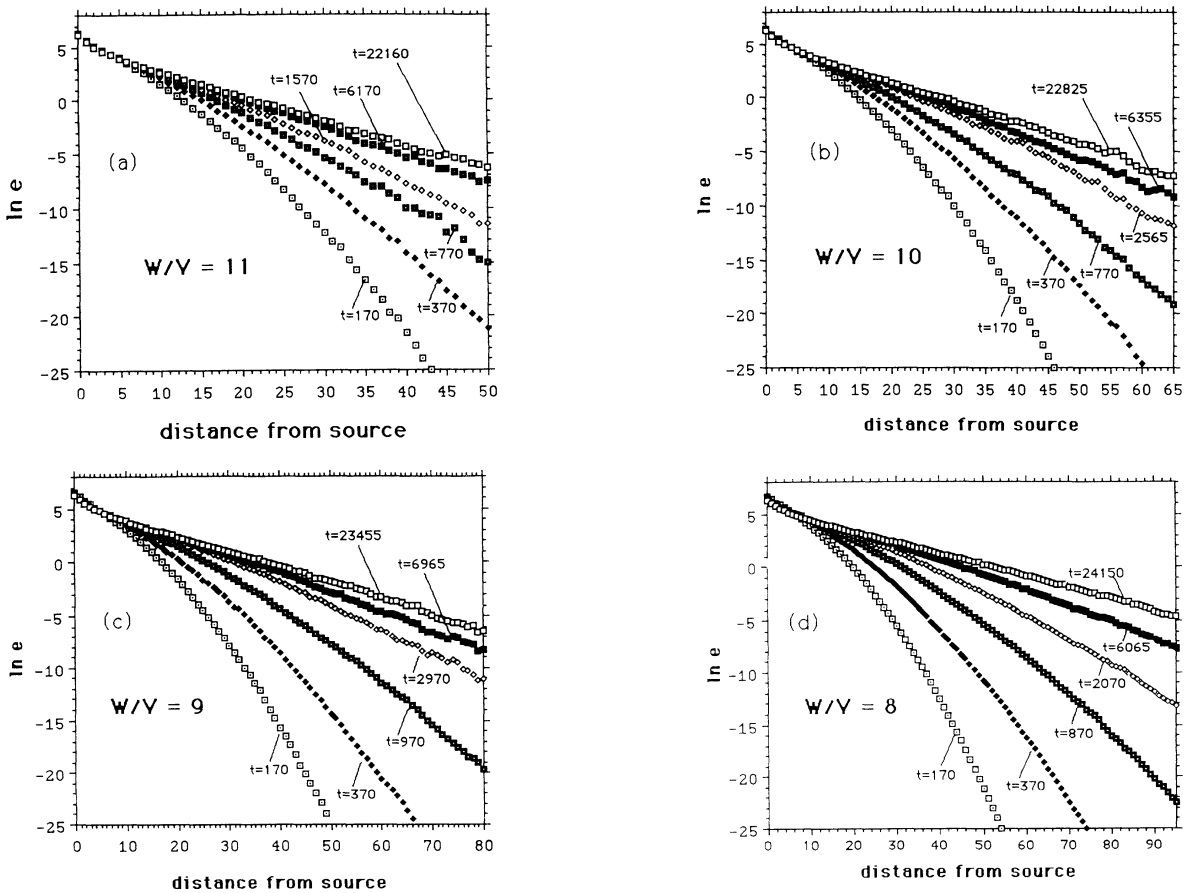

FIG. 4. The spatial profile of the average energy density is exhibited at several different times after the initial energy deposition. (a) $W/V=11$; (b) $W/V=10$; (c) $W/V=9$; and (d) $W/V=8$.

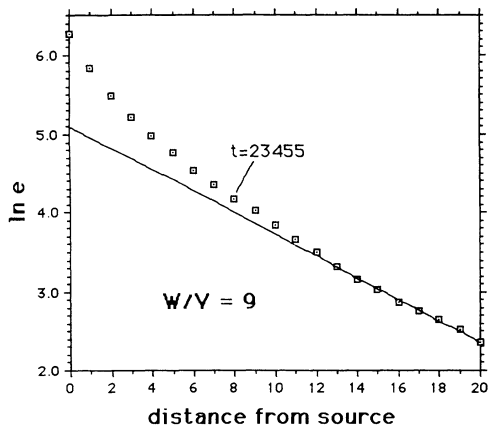

FIG. 5. The energy density profile at $W/V=9$ at very late times and short distances shows a region of enhanced energy density. The energy densities from the numerical simulations are indicated by small squares; the continuous line indicates a linear extrapolation from moderate distances to small distances by means of a slope given by the McKinnon and Kramer localization length.

cribe the peak to a contamination of the disturbance by energies at frequencies associated with localization lengths of the order of the observed widths. Such frequencies are near the band edges, however, and largely unexcited by the tone burst source. The hypothesis is thus incompatible with the observation that the energy associated with the enhancement is a major component (nearly half) of the total disturbance. One might also wish to associate these short length scales with the mean free path. The widths are, however, greater than the mean free path (at all degrees of disorder studied the ensemble average of displacement responses, $\langle v \rangle$, to harmonic forcing has a wavelength of about two lattice spacings and amplitude attenuations of about one power of e per lattice spacing, corresponding to mean free paths of about half a lattice spacing). The enhanced energy density at short distances may perhaps be identified with energy correlation lengths other than ξ such as those noted by others, e.g., McKinnon and Kramer.[25]

The unimportance of the finite geometry was confirmed by repeating the calculation at $W/V=11$ for a total of 250 configurations in an 81×211 mesh. The logarithms of the energy densities in the systems of different sizes were found to agree within statistical uncertainties related to the finite ensemble averaging. Within 8ξ of the source the differences were randomly signed with magnitudes of order 0.15. One concludes that the results presented here are not seriously contaminated by the finite size of the system.

B. R^2 versus time

Numerical experiments[20,21,9,23] in the time domain have in the past chiefly focused upon the particle displacement variance $R^2(t)$, and in particular upon its behavior at late times. This quantity determines the low-frequency limit of what might be called an effective global diffusivity. The self-consistent theory of localization[19] makes an explicit prediction that the real part of that diffusivity is proportional to ω^2. This implies a corresponding prediction for the late time behavior of $R^2(t)$. It should be noted that this theory is based upon a perturbative approach appropriate for a weak-coupling regime, so comparison with measurements in strongly disordered media such as these may be moot.

Generalized diffusivity is defined as the ratio between the energy flux and energy density gradient, each evaluated in the q and ω domains:

$$\sigma(\mathbf{q},\omega) i\mathbf{q}\, e(\mathbf{q},\omega)=\mathbf{j}(\mathbf{q},\omega)\ . \tag{8}$$

Equation (8) is supplemented by the continuity condition,

$$i\omega\, e(\mathbf{q},\omega)=i\mathbf{q}\cdot\mathbf{j}(\mathbf{q},\omega)+Q(\mathbf{q},\omega)\ , \tag{9}$$

where Q is an energy source distribution. By eliminating j from Eqs. (8) and (9), the generalized diffusivity may be found in terms of experimental measurements of energy densities e which are responses to known sources Q.

$$\sigma(\mathbf{q},\omega)=-i\omega/q^2+Q(\mathbf{q},\omega)/\{q^2 e(\mathbf{q},\omega)\}\ . \tag{10}$$

At small q, e is given in terms of R^2 by

$$e(\mathbf{q},t)=\int e(x,t)\cos(qx)\,dx=E_0-q^2E_2(t)/2+\cdots$$
$$=E_0[1-q^2R^2(t)/2+\cdots]\ , \tag{11}$$

or

$$e(\mathbf{q},\omega)=(E_0/i\omega)[1-i\omega q^2R^2(\omega)/2+\cdots]\ . \tag{12}$$

In the present experiments, the energy is deposited in a concentrated and nearly impulsive manner; $Q(\mathbf{q},\omega)=E_0$. Thus one determines

$$\sigma(\mathbf{q},\omega)=-i\omega/q^2[1-\{1-i\omega q^2R^2(\omega)/2+\cdots\}^{-1}]\ , \tag{13}$$

or

$$\sigma(0,\omega)=-\omega^2R^2(\omega)/2\ . \tag{14}$$

If, as is claimed,[19] the real part of $\sigma(0,\omega)$ is proportional to ω^2 as $\omega\to0$, then the only low-ω divergence of $R^2(\omega)$ must be imaginary. Hence the integral,

$$\int_\infty [R^2(\infty)-R^2(t)]\,dt<\infty \tag{15}$$

must exist. This requires R^2 to approach its asymptotic value $R^2(\infty)$ at a rate faster than $1/t$.

To examine this prediction plots of R^2 at late times are shown in Fig. 6. In all of the cases considered the approach to the asymptote appears to be slower than $1/t$. Finite size effects, if any, would presumably have accelerated the approach. Similar slow approaches have been observed by others.[20,21,9,23] One concludes that there is no evidence here for this prediction of the self-consistent theory of localization.

In order to fully characterize wave energy transport in localizing media it is necessary to study other quantities as well as R^2. Indeed, the simple global quantity, R^2,

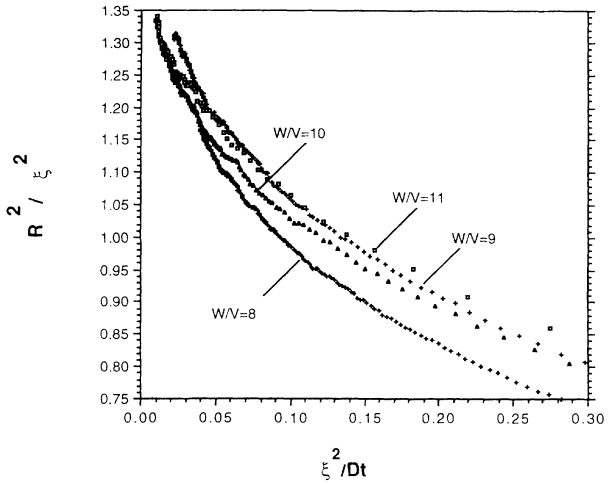

FIG. 6. The particle displacement variance $R^2(t)=E_2/E_0$ is plotted in dimensionless units versus the inverse of time for each of the four degrees of disorder.

while often studied in numerical experiments, is not readily ascertained in laboratory classical wave experiments at fixed source and receiver position. In the remainder of this communication we therefore confine attention to local responses.

C. Temporal behavior versus the logarithm of time

There are a variety of ways in which the temporal behavior might be displayed. Large dynamic range may be obtained in plots of the logarithm of energy density versus the logarithm of time. Such plots are shown in Figs. 7(a)–7(d) for the four degrees of disorder considered here and for four different scaled distances from the source: two, four, six and eight localization lengths. Energy densities were evaluated at fractional distances by means of linear interpolations of their logarithms. Perhaps worthy of first note in these figures is that the transport at large distances is not exponentially slow. That observation may be quantified by associating a transport time scale with the arrival of the disturbance at a position a distance x from the source, and comparing it to the occasionally hypothesized time scale x^2/D where D is an exponentially renormalized diffusion constant. An arrival time may be identified with the time at which the first $1/e$ of the asymptotic value of the energy density has arrived. At $x=6\xi=43.8$, $W/V=9$ this time is $T=\exp(9)\approx 8100$ [Fig. 7(c)]. A time scale x^2/D based on a hypothesized exponentially renormalized diffusion rate $D\approx D_0\exp(-x/\xi)\approx 0.00025$ would be of the order of $x^2/D\approx 7.8\times 10^6$. No times of that magnitude are present in the curve. The absence of exponentially long

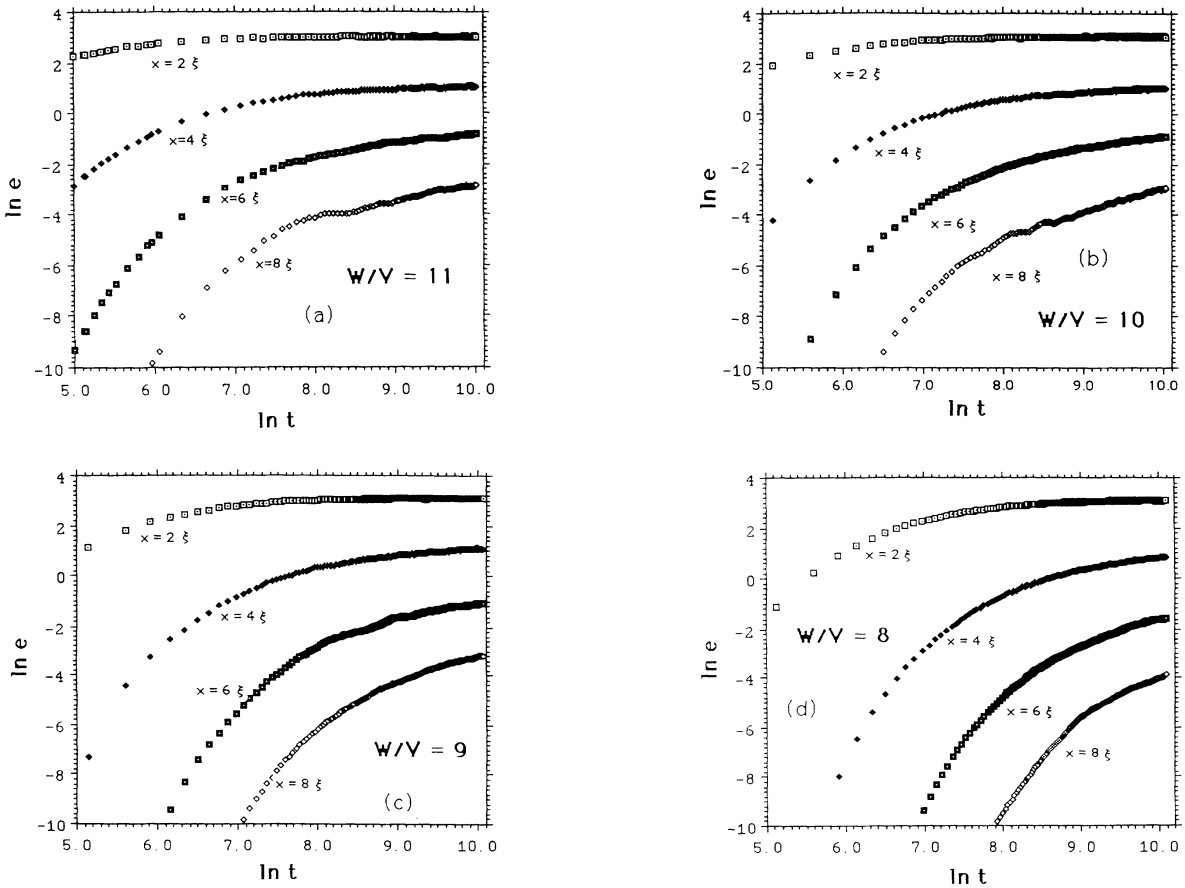

FIG. 7. The temporal behavior of the average energy density is exhibited at four different distances, two, four, six, and eight localization lengths from the source. (a) $W/V=11$; (b) $W/V=10$; (c) $W/V=9$; and (d) $W/V=8$.

times in the energy profiles is consistent with the argument advanced in Ref. 16 that there can be no time scales greater than the modal density. That the concept of exponentially slow diffusion is incorrect has also been argued by Sornette.[28]

The transport behaviors at the different degrees of disorder in Figs. 7 are very similar. Over most of the evolution they are, furthermore, identical to within a rescaling of time. Figure 8 shows a replot of the data of Figs. 7 in which the data from $W/V=8$, 9, 10, and 11 are shifted in (log) time by amounts of $\Delta_1=1.98$, 1.11, 0.47, and 0.00, respectively, in order to collapse the data from different degrees of disorder to a single set of curves. These values of Δ_1 were chosen to effect an optimal collapse, but almost equally good collapse is obtainable with choices for Δ_1 differing by as much as 0.02. Δ_1 should therefore be understood to have at least that much error.

Inasmuch as the evolutions at different degrees of disorder are identical except for the rescaling of time one might say that, for example, the transport at $W/V=8$ is exp(1.98) times slower than the transport at $W/V=11$. Such a comparison is somewhat inapt, however, as the distances over which the transport is acting are different. One may construct dimensional rates by inserting a factor of some power of the distance scales. In the absence of theoretical guidance the choice of a power is a matter of guesswork. The choice of the second power, however, allows one to identify the dimensional rate as a kind of residual diffusivity. One defines a dimensional residual diffusivity relative to the case $W/V=11$ by $\exp(-\Delta_1)(\xi/4.22)^2$ and concludes that the lower disorder cases have residual diffusivities of 0.95, 1.10, and 1.04 (for $W/V=8$, 9, and 10, respectively) times that of the case $W/V=11$. These quantities have units of distance squared per time but appear to be proportional to neither of the two known quantities with these units, not the bare diffusivities given in Table I, nor to the inverses of the modal densities.

It is remarkable that the evolutions at different degrees

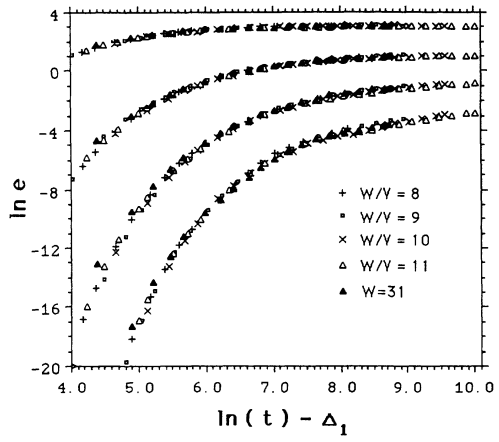

FIG. 8. The data of Figs. 7 are collapsed to a single set of curves, one for each scaled distance from the source, by choosing an optimal rescaling of time for each degree of disorder. The energies from the non-Anderson model at $W=31$ are also found to collapse to the same set of curves.

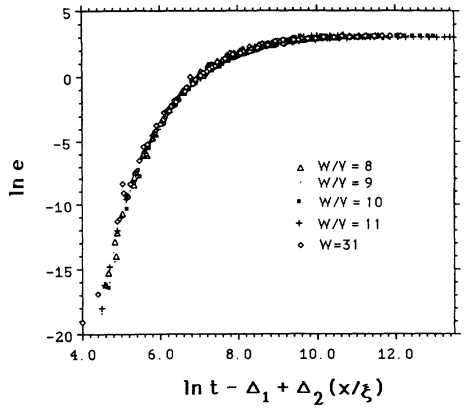

FIG. 9. Twenty sets of data, from all four Anderson models, and the non-Anderson model considered in Sec. V, and all four distances from the source, collapse to a single function.

of disorder scale to each other as well as they do. The implication is that there exists a universal function $E(x/\xi,t/T)$, where T and ξ are microstructure-dependent quantities, which describes transport in Anderson localizing systems. Furthermore, T does not appear to be proportional to either of the more obvious microstructure-dependent quantities which have units of time.

The curves governing the transport process may be further collapsed by applying an additional x/ξ dependent shift in (log) time, again chosen in order to effect an optimal collapse. A factor of $\exp(x/\xi)$ is also applied in order to reconcile the different amplitudes at different distances. The choice of shifts: $\Delta_2=0.0$ for $x=8\xi$, $\Delta_2=0.67$ for $x=6\xi$, $\Delta_2=1.7$ for $x=4\xi$, and $\Delta_2=3.4$ for $x=2\xi$ successfully collapses all the data, from four different distances from the source and all cases of disorder considered, as shown in Fig. 9.

Most interestingly these choices for the further time shift, made in order to effect an optimal collapse, appear to scale with a fractional power of x/ξ as may be seen in Fig. 10, leading one to hypothesize a general, universal character to the transport of an Anderson localizing

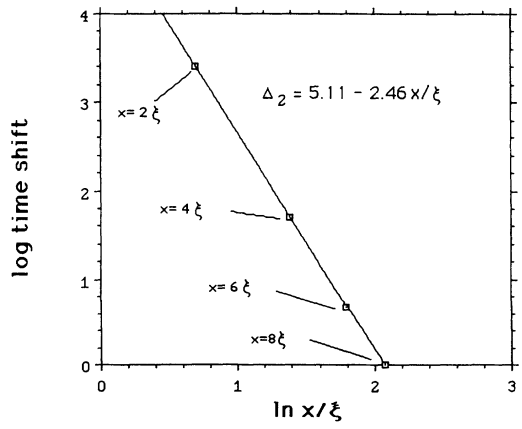

FIG. 10. The collapse shown in Fig. 9 was effected by a time shift proportional to the -2.46 power of x/ξ.

quantity of the form

$$e(x,t)=\exp(-x/\xi)F((x/\xi)^{2+n}\exp\{\Delta_1\}/t)\ ,$$

where n is an anomalous dimension for the diffusivity and appears to be about 0.46 and Δ_1 depends on the microstructure but not on x or t.

D. Temporal behavior versus inverse time

The data may also be plotted versus the inverse of time to reveal an interesting behavior. Such a plot is shown in Fig. 11 for the case $W/V=9$, $x=6\xi$ in which the abscissa is the distance squared over four times the product of time and bare diffusivity.

Classical diffusion from an instantaneous point deposition of energy would behave nearly linearly on such a plot.

$$\ln e(x,t)=\ln E_{\text{total}}-x^2/4Dt-(1/2)\ln(4\pi Dt)\ . \quad (16)$$

However, for depositions such as the present one which are distributed in time, one must convolve the Green's function, Eq. (16), with the known deposition profile. This has been done and is also plotted in Fig. 11. D has been set to the bare diffusivity, 0.105. One can see here that the energy density at the earliest times is approximately classical. Statistically significant deviations from the classical prediction occur at the earliest times (not shown in the figure) and may be ascribed to dispersion—due to frequency dependence—in bare diffusivities. At early times and large distances Eq. (16) is very sensitive to variations in D. Equation (16) averaged over a range of values of D is much greater than Eq. (16) evaluated at the mean D, hence, the discrepancy. A detailed comparison with classical diffusion theory may require the use of a tone burst source with a central frequency at a point such that D_0 is stationary.

By times of the order of $2\xi^2/4D_0$ (or $x^2/4D_0t=18$ if $x=6\xi$) the localization is apparent as the energy density falls below the classical value. At much later times $(x^2/4D_0t<4)$ $(t>3000)$ the behavior approaches a line parallel to the classical line but weaker than it by a factor of the order of $\exp(-x/\xi)$. In this region one may roughly approximate the energy density by the very simple formula: $e(x,t)\approx\exp(-x/\xi-x^2/4D_0t)$. It is noteworthy that time scales at moderately late times and large distances are comparable to classical time scales determined by the diffusivity on the microscale. In this parameter range the transport behavior of an Anderson localizing quantity is approximately that of the corresponding classical quantity except for an exponential diminishment of strength: $\exp(-x/\xi)$.

At the later times the plot in Fig. 11 shows a steepening slope. This behavior is seen also at other degrees of disorder at the larger distances. Such late times may be of only academic interest because in practice, laboratory disturbances at late times will have suffered too much dissipation to be observable. Nevertheless the steepening is intriguing, in part because it suggests that the form $\exp(-x/\xi-x^2/4D_0t)$ is not the correct asymptotic form. In Figs. 12 the very late time behavior at $x=6\xi$ and $x=8\xi$ is shown on an expanded scale for all degrees of disorder. Statistical fluctuations are more apparent on

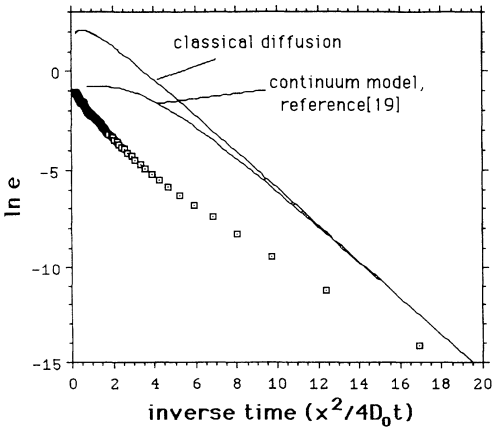

FIG. 11. The observed energies are plotted versus the inverse of time for the case $W/V=9$ and at a distance of six localization lengths from the source ($x=43.8$). Also shown are the predictions of classical diffusion and of the simple continuum model for the transport of an Anderson localizing quantity.

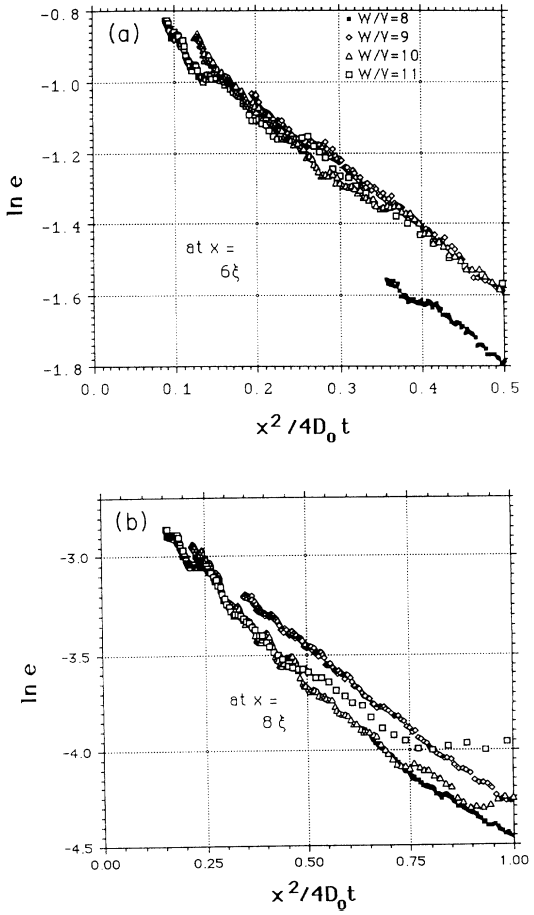

FIG. 12. At $x=6\xi$ (a) and at $x=8\xi$ (b) the average energies are plotted versus the inverse of time at late times for all degrees of disorder.

this expanded scale. Nevertheless it appears as if the slopes are significantly greater than unity for all degrees of disorder and for both distances portrayed.

A hypothesis that the transport is governed at the latest times and larger distances by, not the bare diffusivity, but by the modal density, is not supported by this data. The hypothesis that these energies are functions of time solely by means of the dimensionless quantity $\rho x^2/t = 4\rho D_0 (x^2/4D_0 t)$ would imply that, given that this limit exists, the asymptotic slope would be steeper at the lower amounts of disorder by a factor of the ratio of the products of the ρD_0's, or about 85% steeper at $W/V=8$ than at $W/V=11$. The observed behavior is not consistent with this hypothesis. An hypothesis that the steepening at the latest times is due to domination by components with particularly slow bare diffusivities is also difficult to maintain. The asymptotic slopes shown in Fig. 9 are twice unity. The alternative hypothesis would therefore have to assert that components with bare diffusivities half that of the band center dominate at late

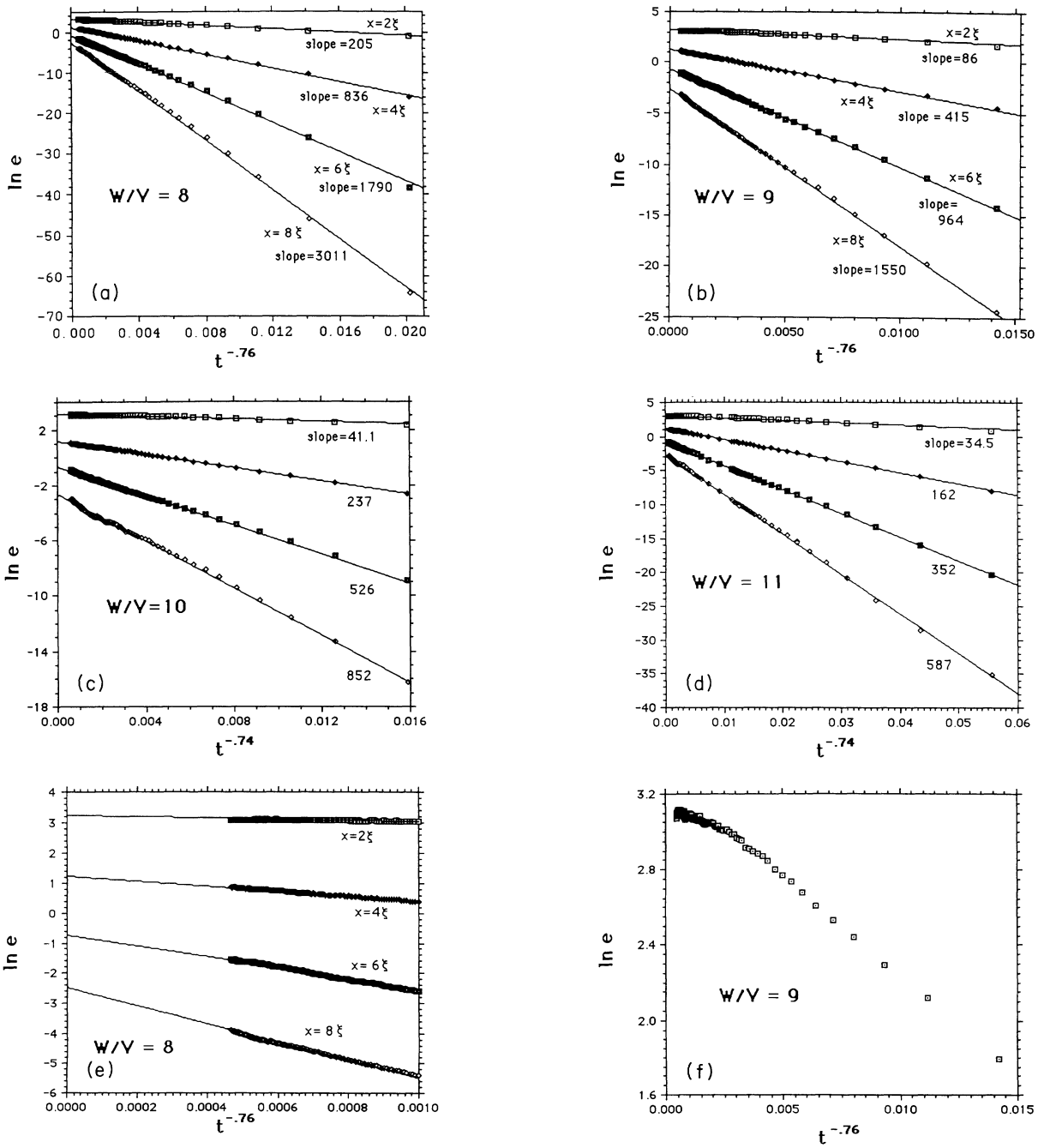

FIG. 13. The logarithms of the average energy densities are found to fit well to linear functions of an inverse fractional power of time. (a) $W/V=8$; (b) $W/V=9$; (c) $W/V=10$; (d) $W/V=11$. The late time behavior is shown on an expanded horizontal scale in (e), and in (f) the behavior at $x=2\xi$ is shown on an expanded vertical scale.

times and large distances. However, components with slow diffusivities are far from the band center and are consequently weakly excited; they, furthermore, presumably have short localization lengths and therefore should not be expected to dominate at large distances.

E. Temporal behavior versus inverse fractional powers of time

Thus the hypothesis that the asymptotic transport of an Anderson localizing quantity is of the form $\exp(-x/\xi - x^2/4D_0t)$ is, at best, only weakly supported by the data. From Sec. IV C, however, it is known that there is a single function of time and distance which describes the evolution of the distribution of the observed energy density. Further guidance may be taken from the observed dependence of time scales on a noninteger power of distance and from the slight, but persistent, curvature in the plots versus the inverse of t. In an attempt to ascertain the correct analytic form for $e(x,t)$, plots versus various fractional inverse powers of t were obtained. The most striking plots were found when the abscissa was chosen to be t^{-p} with $p \approx 0.76$. Shown in Fig. 13(a) is the result of that plot for the case $W/V=8$. Also shown are linear fits to the data points.

The high quality of the linear fits, over two orders of magnitude in time and 26 in energy suggests that the linearity is not an accident. Figures 13(b)–13(d) show similar plots for other degrees of disorder. The data, and the fits, at the latest times are shown on an expanded scale in Fig. 13(e) where it may be observed that the steepening seen in Fig. 11 has now been absorbed into the fractional power of time. One is led to a conjecture, supported by the current data, but in need of refinement and corroboration. Transport of an Anderson localizing quantity in two dimensions is given, at times after the domain of classical diffusion, by the following formula:

$$e(x,t)=\exp\{-x/\xi-(x^{2+n}/4\beta\xi^n t)^p\}\ , \tag{17}$$

where $n \approx 0.5$, $p \approx 0.75$, and β is a microstructurally determined residual diffusivity proportional to neither D_0 nor $1/\rho$. The values of n, p, and β corresponding to the curves judged to best fit Eq. (17) to the data at $x=4\xi$, 6ξ, and 8ξ are shown in Table I.

The data from $x=2\xi$ was excluded from the fit. At late times and small distances, as may be seen in Fig. 13(f), the behavior indicated by Eq. (17) is modified by a rolloff with a magnitude that may be of the order of a part in $\exp(x/\xi)$. This correction to (17) will not be explored here. One may note, though, that similar rolloffs related to the $\log(t)$ term in Eq. (16) occur in classical diffusion also. As in the classical case, the rolloff here may correspond to the loss of energy at a position x due to further energy transport to points beyond x.

It may well be imagined that the dispersion in transport properties implicit in the average over frequencies in the tone burst source can make precise evaluations of n, p, and β (and ξ) difficult. The quantities quoted in Table I are thus subject to uncertainty. New experiments, designed with a minimum of such dispersion, may be necessary before more exact estimations of transport parameters can be made.

Equation (17) cannot be exact, as it neither exhibits classical behavior at early times, nor conserves the spatial integral of energy density, nor exhibits the region of enhanced energy density near the source. Neither does (17) predict the rolloff seen in Fig. 13(f). Equation (17) also violates the constraint suggested by Weaver[16] that time scales at a distance x cannot exceed some multiple of ρx^2. It is nevertheless a viable and intriguing candidate for an approximate mean energy density propagator and well supported by the data.

V. BEHAVIOR OF A DIFFERENT DISORDERED SYSTEM

In order to explore the generality of the behavior seen above an alternative microstructure was studied as well. A modification of the system described by Eqs. (1) was considered which includes coupling to next-nearest neighbors:

$$\partial^2 v_{\mathbf{n}}/\partial t^2 + k_{\mathbf{n}} v_{\mathbf{n}} - \sum v_{\mathbf{m}} - 2\sum v_{\mathbf{m}} = F_{\mathbf{n}}(t) \tag{18}$$

where the first sum is over all nearest neighbors $\mathbf{m}$ to $\mathbf{n}$, the second sum is over all next-nearest neighbors, and $k_{\mathbf{n}}$ is taken to be 13 plus a random number from the uniform distribution $[0,W]$. This system has greater coupling (coordination number equal to 8 now instead of 4 and a larger value of V) so one expects longer localization lengths for the same values of W. The forcing was again a 30 cycle tone burst at a frequency of $(5+W/2)^{1/2}$, modified as before by a finite time step $\delta t=(12.5+W)^{-1/2}$. The forcing frequency is not, in this case, at the band center.

At $W=31$ the early time behavior in this system indicates a bare diffusivity D_0 of 0.207. The average spectrum of 20 realizations of a 10×10 version of this system was found to have a modal density of 0.235 (modes per site per apparent circular frequency). Extrapolation of the late time behavior shown in Fig. 14 to infinite time indicates a localization length estimate of $\xi \approx 6.0$.

At short distances the energy density at late times is enhanced above the point which would be obtained by extrapolation of the data from moderate distances back to

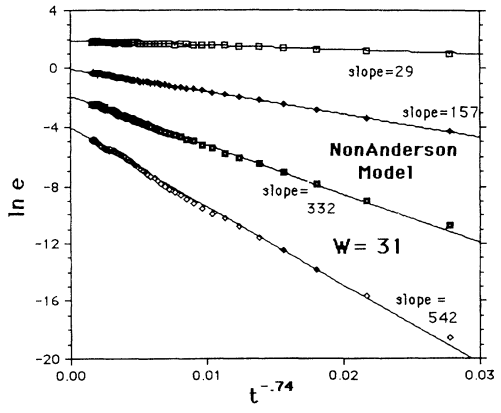

FIG. 14. The energy densities from the non-Anderson model are also found to fit to linear functions of an inverse fractional power of time.

the source. The enhancement is by a factor of about 3.0. The enhancement is $\sqrt{3}$ at $x \approx 2.25$. Thus this feature in the profiles from the Anderson model is also found in the profile from the model with a different microstructure.

Figures 7 and 8 in which the Anderson model system behavior was shown to collapse to a disorder-independent set of curves also show the collapse of this other model, after a choice of time shift, $\Delta_1 = -0.05$. This value of Δ_1 corresponds to a dimensional residual diffusivity relative to that of the case $W/V = 11$ which is $\exp(0.05)(6.0/4.22)^2 = 2.12$ times faster. The linear fits shown in Fig. 14 indicate that the evolution of energy density in this system is also well approximated by Eq. (17). Values for β, n, and p for those fits are shown in Table I.

VI. COMPARISON TO A HYDRODYNAMICAL CONTINUUM MODEL

Vollhardt and Wolfle[19] have suggested a simple effective continuum description for a diffusely transported Anderson localizing quantity. In this model one asserts an equation of continuity relating particle (or energy) flux $\mathbf{j}$, particle (or energy) density e, and a source term Q:

$$\partial e/\partial t + \nabla \cdot \mathbf{j} = Q \ , \tag{19}$$

being the space-time version of Eq. (9). One also hypothesizes a constitutive relationship,

$$\partial^2 \mathbf{j}/\partial t^2 + \alpha \nabla \partial e/\partial t = (-1/\tau)\partial \mathbf{j}/\partial t - \omega_0^2 \mathbf{j} \ , \tag{20}$$

in which flux is driven by density gradient, and restrained by an "oscillator strength" ω_0^2. The term in $1/\tau$ represents a viscous friction and τ may be interpreted as a time scale over which ballistic flux is attenuated.

These equations may be Fourier analyzed in time and space and the response in an initially quiescent system found to be

$$e(\mathbf{q},\omega) = Q(\mathbf{q},\omega)\frac{i\omega + 1/\tau + \omega_0^2/i\omega}{-\omega^2 + i\omega/\tau + \omega_0^2 + \alpha q^2} \ . \tag{21}$$

If the time scales of interest greatly exceed τ then we may neglect $\omega\tau$ in comparison to unity and approximate e as

$$e(\mathbf{q},\omega) = Q(\mathbf{q},\omega)[1 + \omega_0^2\tau/i\omega]/[i\omega + (\alpha q^2 + \omega_0^2)\tau] \ . \tag{22}$$

At late times ($\omega \to 0$) the energy density becomes

$$e \approx [Q(q,\omega)/i\omega]/[1 + \alpha q^2/\omega_0^2] \ , \tag{23}$$

or, if $Q(x,t) = \delta(x)\delta(t)$, then as $t \to \infty$,

$$e(x,t) \to (\sqrt{\alpha}/2\omega_0)\exp\{-|x|\omega_0/\sqrt{\alpha}\} \ . \tag{24}$$

At this point one identifies $(\sqrt{\alpha})/\omega_0$ as the localization length ξ. One further identifies the quantity $(\omega_0^2\tau)^{-1}$ as a time scale T. At early times ($\omega \gg 1/T$) the energy density (22) becomes

$$e(\omega,q) = 1/(i\omega + \alpha\tau q^2) \ , \tag{25}$$

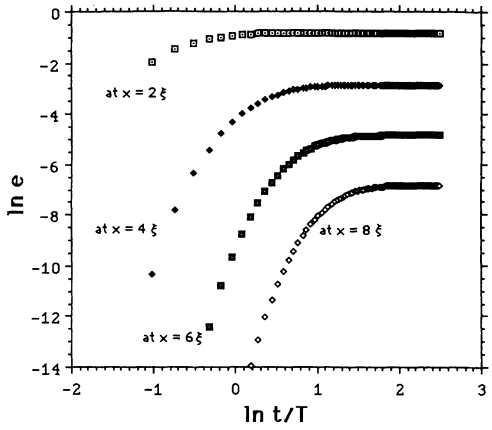

FIG. 15. The evolution of the energy densities according to the simple continuum model, Eq. (20).

which may be identified as a classical diffusion propagator with diffusivity $\alpha\tau = \xi^2/T$.[29]

The inverse ω-Fourier transform of (22) may be carried out analytically by residues: the resulting inverse q-Fourier transform can the be done numerically. The results from the inversion are plotted in Fig. 15. The profiles of Fig. 15 are very clearly not like those of Figs. 7; they cannot be made to collapse to the curves shown in Fig. 7 by any simple rescaling of time. Nor can this be done by confining attention to the latest of times for which the theory[19] is presumably intended; the observed approaches to the late time asymptote are far slower than theory would predict. This was also noted in Sec. IV B.

The energy density at $x = 6\xi$ as predicted by the continuum model (22) is also plotted in Fig. 11. The simple continuum model predicts evolutions that are close to their classical counterparts until late times of the order of $x\xi/4D_0$, thereby resulting in a much more rapid completion of transport than is observed in the data. The late deviation may be compared to the early deviation observed in the present experiments, at times no later than $\xi^2/4D_0$. One concludes that the predictions of the simple continuum model are contradicted by the data. This was also observed in Weaver's ultrasonic experiments.[12] An alternative continuum model is required.

VII. THE EFFECT OF DAMPING

It has been long believed that dissipation in classical wave systems provides unique difficulties for experiments designed to detect localization. For this reason the effects of dissipation on localization have received significant theoretical attention.[1,2,16,28] In accord with expectations, dissipation has complicated the analysis of some experiments[10,11] and limited signal durations in others.[12] It may be inescapable in the laboratory search for localization of classical waves. Its effect on $e(x,t)$ is therefore of great importance.

There is a widespread conception that dissipative, but otherwise localizing, systems will behave diffusively. A previous communication,[16] however, argued and demonstrated that viscous dissipation has no effect upon energy density profiles beyond the trivial: $e(x,t)$ gaining a fac-

tor $\exp(-st)$ where s is a mean energy dissipation rate. The numerical demonstration there was, however, conducted on systems of small size. In this section the evolution in large damped systems is presented in order to determine whether the result found in Ref. 16 is size dependent.

As in Ref. 16, Eq. (1) is modified to include a viscous dissipation term

$$\partial^2 \underline{v}(t)/\partial t^2 + \underline{\underline{C}}\partial \underline{v}(t)/\partial t + \underline{\underline{K}}\underline{v}(t) = \underline{F}(t) , \tag{26}$$

where $\underline{\underline{C}}$ is a diagonal matrix with elements chosen randomly and independently from the uniform distribution from zero to $2s$.

The equation is solved, as before, by an explicit central difference method. For the case $s = D_0/\xi^2 = 0.0045$ at $W/V = 11$, $e(x,t)$ is shown in Fig. 16. The exponential spatial gradient in energy density is maintained in the presence of damping. Hence the earlier conclusions[16] are corroborated: dissipation does not alter the energy transport properties except in a trivial manner. In particular, introduction of dissipation into a localized system does not induce classical diffusion.

It is noteworthy that the rate of energy absorption, $-\partial \ln e/\partial t$ diminishes at the later times. Behavior like this was not observed in Ref. 16. It is, however, often seen in room acoustics[30] and is often related to the presence of a distribution $p(s)$ of modal dissipation rates: at late times the less dissipated modes have preferentially survived and then dominant the decay. One may estimate the width of the distribution $p(s)$ by assuming s to be given by $\underline{\psi}^T \underline{\underline{C}} \underline{\psi}$ where $\underline{\psi}$ is an eigenmode. If a typical localized mode has significant access to only ξ^2 sites then s is the sum of the squares of ξ^2 random numbers. Thus s should be distributed with a χ-square distribution. This reasoning was found to precisely predict the curvature seen at $x = 0$. Therefore the curvature is ascribed here to that effect. It is not a sign of any dissipation-induced cutoff in a renormalization of diffusivity.

It is interesting that the curves associated with the larger distances have less curvature. Smaller curvature implies that the modes responsible for transport over the larger distances have significant access to a number of sites greater than ξ^2. The modes responsible for the transport are, perhaps, atypical.

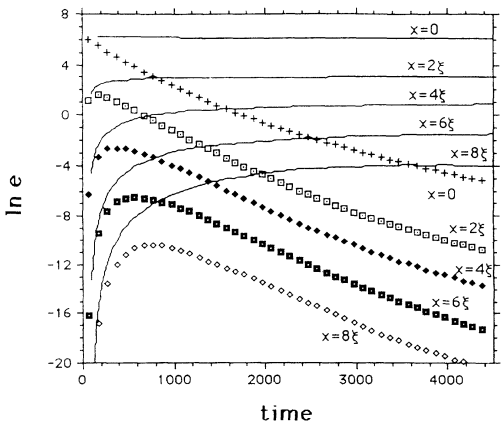

FIG. 16. The evolution of the energy density in a damped system at $W/V = 11$ for five different distances from the source (discrete plot symbols) is compared to that of the undamped case (solid lines).

VIII. CONCLUSIONS

Numerical experiments have unambiguously demonstrated several properties of wave energy transport in two-dimensional disordered media. Amongst these one may count the clear evidence that the asymptotic approach to the condition of simple exponential spatial decay is slower than would have been predicted by a simple hydrodynamical continuum model or by standard theory for the weak disorder limit, and much faster than would have been anticipated by appeal to common expressions for the renormalization of diffusion rates. It has shown that dissipation does not delocalize otherwise localizing systems. The existence of length scales less than the localization length and important for short source-receiver separations has also been demonstrated.

At early times $e(x,t)$ is consistent with predictions of classical diffusion and may be used to define a bare diffusivity D_0. Deviations signaling the onset of localization occur by times of the order of $\xi^2/4D_0$, even for large x. The evolution of energy density thereafter is not classically diffusive, nevertheless, at the moderate distances and times investigated, the time scale of the transport process was found to be of the same order as that which one would have in the absence of localization: $T \approx x^2/4D_0$.

The evolution has furthermore been found, after a disorder and distance dependent rescaling of time, to be independent of the degree of disorder and of the form of the wave equation on the microscale. The data suggests that transport at times beyond $\xi^2/4D_0$ and distances beyond 2ξ is governed by a universal formula approximatable by

$$e(x,t) = \exp\{-x/\xi - (x^{2+n}/4\beta\xi^n t)^p\} , \tag{27}$$

where β may be termed a residual diffusivity. β is presumably microstructurally determined but it does not appear to be equal to the bare diffusivity.

This report has left many questions unanswered and raised new ones. Amongst those unaddressed one may count the issue of the isotropy of transport in the Anderson model, and the effect of boundary conditions, both reflective and radiative boundaries being relevant to experiments and unexamined by these experiments. Future work should attempt to quantify the transition from classical to localized behavior, as these early times are highly relevant to dissipative laboratory systems. Greater clarity may be obtained if future numerical experiments are conducted at frequencies at which D_0 and/or ξ are stationary. Future work should also attempt to evaluate the detailed quality of the data collapse and the associated universality: is in fact the behavior independent of microstructure except inasmuch as the microstruture may determine two transport parameters—a localization length and a single residual diffusivity?

Perhaps the most obvious extension of this work would be to three dimensions. The present calculations required a few times 10^{13} floating point operations and a direct extension to three dimensions would require about one hundred times as much computation. In the absence of methods for improving computational efficiency an extension to three dimensions would not be a simple matter. It may be hoped that computations in two dimensions will sufficiently inform the theorist's search for an effective continuum model for transport in Anderson localizing systems that predictions for three-dimensional laboratory systems may be forthcoming.

ACKNOWLEDGMENTS

The author thanks Dr. Tarek Shawki for access to his HP Apollo 9000 workstation and the thousand CPU hours needed to carry out these calculations. This work was supported by the National Science Foundation through Grant No. MSS 91 14360. Thanks are also due to the Materials Science Center and the Department of Theoretical and Applied Mechanics at Cornell University for use of their facilities.

[1]P. W. Anderson, Philos. Mag. B **52**, 505 (1985).
[2]S. John, Phys. Rev. Lett. **53**, 2169 (1984); Phys. Rev. B **31**, 304 (1985).
[3]T. R. Kirkpatrick, Phys. Rev. B **31**, 5746 (1985).
[4]C. A. Condat, J. Accoust. Soc. Am. **83**, 441 (1988).
[5]R. Weaver, Int. J. Eng. Sci., **22**, 1149 (1984).
[6]C. M. Soukoulis, E. N. Economou, G. S. Grest, and M. H. Cohen, Phys. Rev. Lett. **62**, 575 (1989).
[7]*Scattering and Localization of Classical Waves in Random Media,* edited by P. Sheng (World Scientific, Singapore, 1990).
[8]C. H. Hodges, J. Sound Vib. **82**, 411 (1982).
[9]M. Kaveh, Philos. Mag. B **56**, 693 (1987).
[10]A. Z. Genack and N. Garcia, Phys. Rev. Lett. **66**, 2064 (1991).
[11]N. Garcia and A. Z. Genack, Phys. Rev. Lett. **66**, 1850 (1991).
[12]R. L. Weaver, Wave Motion **12**, 129 (1990).
[13]S. He and J. Maynard, Phys. Rev. Lett. **57**, 3171 (1986).
[14]G. Cody, L. Ye, M. Zhou, P. Sheng, and A. Norris, in *Photonic Band Gaps and Localization,* edited by C. M. Soukoulis (Plenum, New York, 1993), pp. 339–353.
[15]M. P. Van Albada, M. B. van der Mark, and A. Lagendijk, Phys. Rev. Lett. **58**, 361 (1987).
[16]R. Weaver, Phys. Rev. B **47**, 1077 (1993).
[17]B. White, P. Sheng, Z. Q. Zhang, and G. Papanicolaou, Phys. Rev. Lett. **59**, 1918 (1987).
[18]E. Abrahams and P. Lee, Phys. Rev. B **33**, 683 (1986).
[19]D. Vollhardt and P. Wolfle, Phys. Rev. Lett. **45**, 842 (1980).
[20]P. Prelovsek, Phys. Rev. B **18**, 3657 (1978).
[21]G. M. Scher, J. Non-Cryst. Solids **59**, 33 (1983).
[22]H. Shore and J. W. Halley, Phys. Rev. Lett. **66**, 205 (1991).
[23]R. Weaver and J. H. Loewenherz, in *Elastic Wave Propagation,* Proceedings of the IUTAM Symposium, Boulder, Colorado, 1989, edited by S. K. Datta, J. D. Achenbach, and Y. S. Rajapakse (Elsevier, New York, 1990), pp. 459–461.
[24]C. Vanneste, P. Sebbah, and D. Sornette, Europhys. Lett. **17**, 715 (1992).
[25]A. McKinnon and B. Kramer, Z. Phys. B **53**, 1 (1983).
[26]Responses to spatially incoherent force distributions were found to be essentially identical.
[27]For noninfinitesimal δt, the total energy E_0 is not precisely constant. It does, though, have bounded fluctuation. The fluctuation may be largely eliminated by considering only quantities which have been averaged over one cycle of the mean frequency.
[28]D. Sornette, J. Stat. Phys. **56**, 669 (1989).
[29]Vollhardt and Wolfle intended this model to describe only the behavior on the longest time scales. Within the context of that theory therefore, the identification of $\alpha\tau$ with a bare diffusivity is unwarranted. The identification is, however, allowed within a more general context in which Eq. (20) is the hypothesized generalization of the constitutive law of classical diffusion.
[30]K. Bodlund, J. Sound Vib. **73**, 19 (1980).